

Synthesis and property of BrCCH- and BrCCBr-coordinated tetrairon clusters

Masaaki Okazaki ^{a,*}, Masato Takano ^b, Ken-ichi Yoshimura ^a

^a International Research Center for Elements Science, Institute for Chemical Research, Kyoto University, Gokasyo Uji, Kyoto 611-0011, Japan

^b Department of Chemistry, Graduate School of Science, Tohoku University, Sendai 980-8578, Japan

Received 31 January 2005; received in revised form 12 March 2005; accepted 2 May 2005

Available online 24 June 2005

Abstract

The reaction of $(\eta^5\text{-C}_5\text{H}_4\text{Me})_4\text{Fe}_4(\text{HCCH})_2$ (**1**) with 1 equiv. of *N*-bromosuccinimide (NBS) gives the one-electron oxidized form in 83% yield. Further treatment of $[\mathbf{1}]^+$ with NBS results in the stepwise bromination of four acetylenic protons to give $[(\eta^5\text{-C}_5\text{H}_4\text{Me})_4\text{Fe}_4(\text{HCCH})(\text{HCCBr})]^+$ ($[\mathbf{2}]^+$), $[(\eta^5\text{-C}_5\text{H}_4\text{Me})_4\text{Fe}_4(\text{HCCBr})_2]^+$ ($[\mathbf{3a}]^+$), $[(\eta^5\text{-C}_5\text{H}_4\text{Me})_4\text{Fe}_4(\text{HCCBr})(\text{BrCCBr})]^+$ ($[\mathbf{4}]^+$), and $[(\eta^5\text{-C}_5\text{H}_4\text{Me})_4\text{Fe}_4(\text{BrCCBr})_2]^+$ ($[\mathbf{5}]^+$) in moderate yields, with the isomer of $[\mathbf{3a}]^+$, $[(\eta^5\text{-C}_5\text{H}_4\text{Me})_4\text{Fe}_4(\text{HCCH})(\text{BrCCBr})]^+$ ($[\mathbf{3b}]^+$), formed as a minor product. These compounds are characterized by analytical and spectroscopic techniques, and the molecular structures of $[\mathbf{2}](\text{PF}_6)$, $[\mathbf{4}](\text{TFPB})$, and $[\mathbf{5}](\text{TFPB})$ are established by X-ray diffraction analysis [TFPB = tetrakis{bis(3,5-trifluoromethyl)phenyl}borate]. The compounds are confirmed to retain the butterfly core of four iron atoms as in $[\mathbf{1}](\text{TFPB})$. The bromoacetylene part in $[\mathbf{2}]^+$ exhibits high reactivity toward various nucleophiles: Cluster $[\mathbf{2}]^+$ is moisture-sensitive and is converted to a mixture of $[(\eta^5\text{-C}_5\text{H}_4\text{Me})_4\text{Fe}_4(\text{HCCH})(\mu_3\text{-CH})(\mu_3\text{-CO})]^+$ ($[\mathbf{6}]^+$) and $[\mathbf{1}]^+$. Reactions of $[\mathbf{2}]^+$ with ZnR_2 (R = Me, Et) give $[(\eta^5\text{-C}_5\text{H}_4\text{Me})_4\text{Fe}_4(\text{HCCH})(\text{HCC-R})]^+$ in good yields (R = Me ($[\mathbf{9}]^+$), 88%), Et ($[\mathbf{10}]^+$), 91%). Accordingly, treatment of $[\mathbf{2}]^+$ with $\text{HC}\equiv\text{CMgBr}$ and LiS^tTol leads to the introduction of the ethynyl and thiolate groups to give $[(\eta^5\text{-C}_5\text{H}_4\text{Me})_4\text{Fe}_4(\text{HCCH})(\text{HCC-C}\equiv\text{CH})]^+$ ($[\mathbf{11}]^+$), 95% and $[(\eta^5\text{-C}_5\text{H}_4\text{Me})_4\text{Fe}_4(\text{HCCH})(\text{HCC-S}^t\text{Tol})]^+$ ($[\mathbf{12}]^+$), 78%, respectively. Substitution of the bromo group in $[\mathbf{2}]^+$ with pyridine affords $[(\eta^5\text{-C}_5\text{H}_4\text{Me})_4\text{Fe}_4(\text{HCCH})(\text{HCC-Py})]^{2+}$ ($[\mathbf{13}]^{2+}$) in 90% yield. The reaction with 4,4'-bipyridyl (bpy) requires the severer conditions (70 °C, 2 days), probably due to the relative low basicity of bpy, giving $[(\eta^5\text{-C}_5\text{H}_4\text{Me})_4\text{Fe}_4(\text{HCCH})(\text{HCC-bpy})]^{2+}$ ($[\mathbf{14}]^{2+}$) in 54% yield. The substitution reaction with 4,4'-bipyridyl is strongly accelerated by treatment with silver salt to give $[\mathbf{14}]^{2+}$ in 90% yield. The products derived from $[\mathbf{2}]^+$ and nucleophiles are unequivocally determined by elemental, spectroscopic, and X-ray diffraction analyses.

© 2005 Elsevier B.V. All rights reserved.

Keyword: Transition-metal carbon clusters

1. Introduction

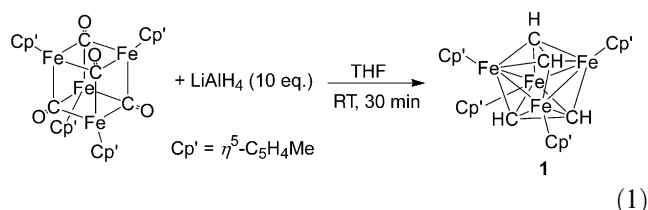
Haloalkynes have been recognized as useful C_2 synthetic intermediates in organic chemistry [1]. However, the coordination chemistry of haloalkynes has yet to

be explored in detail [2]. Most haloalkyne-coordinated complexes are synthesized through a substitution reaction between transition-metal complexes and haloalkynes. For example, $[\text{WCl}_4(\text{BrC}\equiv\text{CBr})_2]$ is formed by the reaction of $\text{BrC}\equiv\text{CBr}$ with WCl_6 in the presence of C_2Cl_4 in boiling carbon tetrachloride [2b], and the treatment of $\text{Pt}(\text{PPh}_3)_4$ with $\text{ClC}\equiv\text{CCl}$ at -30 °C affords $\text{Pt}(\text{ClC}\equiv\text{CCl})(\text{PPh}_3)_2$ in good yield, which can be further converted to *trans*- $\text{PtCl}(\text{C}\equiv\text{CCl})(\text{PPh}_3)_2$ in

* Corresponding author. Tel.: +81774383026; fax: +81774383039.
E-mail address: mokazaki@scl.kyoto-u.ac.jp (M. Okazaki).

boiling toluene [2d]. For M_n transition-metal clusters ($n > 2$), only one example of synthesis has been reported, in which $Cp^*CoFe_3(CO)_9(\mu_4-\eta^2-FC\equiv CF)$ was obtained by irradiating a mixture of $Fe_3(CO)_9-(\mu_3-CF)_2$ and $Cp^*Co(CO)_2$ [2e]. The reactivity of these complexes and clusters thus remains largely unknown.

Recently, our group successfully realized the transformation of four carbon monoxide molecules to two acetylene molecules on the tetrairon core (Eq. (1)) [3]. The next step is to convert the resulting acetylene moieties to haloacetylene and dihaloacetylene, which are expected to be useful intermediates for the functionalization of acetylene. This article presents the stepwise bromination of two acetylene ligands in $[(\eta^5-C_5H_4Me)_4Fe_4(HCCH)_2]^+$ (**[1]**⁺) using *N*-bromosuccinimide (NBS) to form $[(\eta^5-C_5H_4Me)_4Fe_4(HCCH)(HCCBr)]^+$ (**[2]**⁺), $[(\eta^5-C_5H_4Me)_4Fe_4(HCCBr)_2]^+$ (**[3a]**⁺), $[(\eta^5-C_5H_4Me)_4Fe_4(HCCBr)(BrCCBr)]^+$ (**[4]**⁺), and $[(\eta^5-C_5H_4Me)_4Fe_4(BrCCBr)_2]^+$ (**[5]**⁺). The resulting bromoacetylene- and dibromoacetylene-coordinated clusters are characterized by elemental, spectroscopic, and X-ray diffraction analyses. The bromoacetylene part in $[(\eta^5-C_5H_4Me)_4Fe_4(HCCH)(HCCBr)]^+$ (**[2]**⁺) displays high reactivities toward a variety of nucleophiles such as water, ZnR_2 ($R = Me, Et$), $HC\equiv CMgBr$, LiS^pTol , pyridine, and 4,4'-bipyridyl. A part of this work has been reported as a preliminary form [4].



2. Results and discussion

2.1. Bromination of acetylenic protons in $(\eta^5-C_5H_4Me)_4Fe_4(HCCH)_2$ (**1**)

2.1.1. Reaction of $(\eta^5-C_5H_4Me)_4Fe_4(HCCH)_2$ with NBS

Treatment of $(\eta^5-C_5H_4Me)_4Fe_4(HCCH)_2$ (**1**) with 1 equiv. of NBS afforded $[(\eta^5-C_5H_4Me)_4Fe_4(HCCH)_2]Br$ (**[1]Br**) in 83% yield (Eq. (2)), in which NBS operated as an oxidant. Complex **[1]Br** was characterized by elemental analysis and by comparison of nuclear magnetic resonance (NMR) data with the data reported previously for **[1](OTf)** [3b]. In the reaction mixture, no products derived from bromination of the acetylenic protons could be detected.



Treatment of the isolated one-electron cationic form **[1](OTf)** with NBS resulted in the formation of $[(\eta^5-C_5H_4Me)_4Fe_4(HCCH)(HCCBr)](OTf)$ (**[2](OTf)**, 91%) and succinimide (82%) (Scheme 1). Further treatment with NBS led to the stepwise bromination of two acetylene ligands to give $[(\eta^5-C_5H_4Me)_4Fe_4(BrCCBr)_2](OTf)$ (**[5](OTf)**). All clusters were isolated in moderate yields. **[2](PF₆)** and **[2](TFPB)** [TFPB = tetrakis{bis(3,5-trifluoromethyl)phenyl}borate] were obtained by similar methods. The formulas for clusters **[2]**⁺–**[5]**⁺ were established by elemental analysis. As expected from the odd number of cluster electrons, the ¹H NMR signals exhibit characteristic paramagnetic shifts and line broadening. The NMR data for the acetylenic protons in **[1]**⁺–**[4]**⁺ are listed in Table 1. The increase in the number of

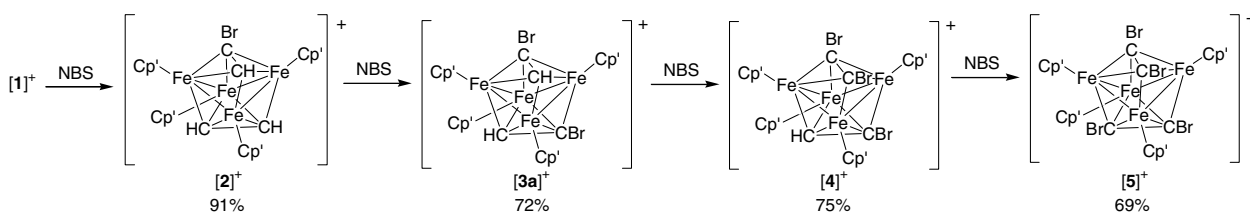
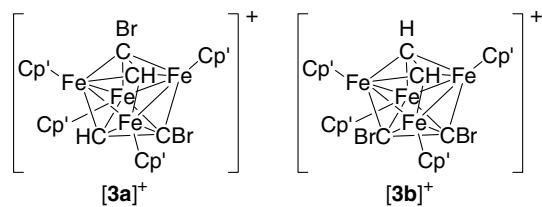


Table 1
¹H NMR data (CD₃CN) of the acetylenic protons in **[1]**⁺–**[4]**⁺ and **[9]**⁺–**[14]**²⁺

Nu		[1] ⁺	[2] ⁺	[3a] ⁺	[3b] ⁺	[4] ⁺	[9] ⁺ Me	[10] ⁺ Et	[11] ⁺ C≡CH	[12] ⁺ S ^p Tol	[13] ²⁺ py	[14] ²⁺ bpy
HCCH	δ	−75.0	−70.6	–	−67.4	–	−72.8	−71.4	−72.8	−68.0	−69.8	−70.2
HCCBr	δ	–	−61.0	−57.2	–	−54.0	–	–	–	–	–	–
HCC–Nu	δ	–	–	–	–	–	−76.3	−79.9	−67.1	−71.4	−52.6	−52.9



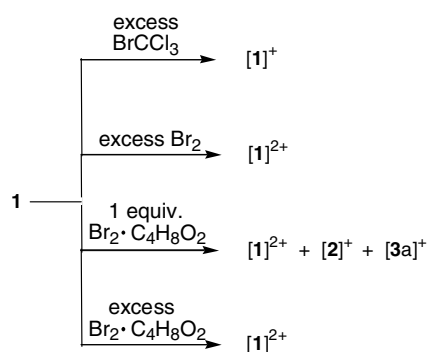
Scheme 2.

introduced bromines leads to a downfield shift of the acetylenic protons. This tendency is attributable to the diamagnetic deshielding effect of bromine.

For the clusters of type $[(\eta^5\text{-C}_5\text{H}_4\text{Me})_4\text{Fe}_4(\text{C}_4\text{H}_2\text{-Br}_2)]^+$, two isomers $[3a]^+$ and $[3b]^+$ can be considered, as illustrated in Scheme 2. Although both isomers possess two sets of chemically equivalent iron centers, the two can be distinguished by NMR spectroscopy on the basis of the chirality around the iron center. The ^1H NMR spectrum of the isolated product displays eight signals at δ 1.0 (2H), 4.1 (2H), 7.1 (2H), 9.6 (2H), 10.2 (2H), 10.9 (2H \times 2, accidentally overlapped), 11.0 (2H), assigned to the ring protons of the $\eta^5\text{-C}_5\text{H}_4\text{Me}$ ligands, which is in good agreement with the structure of $[3a]^+$ possessing two sets of chiral iron centers. ^1H NMR monitoring of the reaction of $[2]^+$ with 1 equiv. of NBS confirmed that $[3b]^+$ was formed as a minor product. The molar ratio of $[3a]^+$ to $[3b]^+$, determined from the ^1H NMR spectrum, was approximately 3:1. Thus, besides the signals of $[3a]^+$, the ^1H NMR spectrum of the reaction mixture displayed four signals assignable to $\text{C}_5\text{H}_4\text{Me}$ ring protons, supporting the formation of $[3b]^+$ with two sets of achiral iron centers. A singlet signal was also observed at δ -67.4, assigned to protons of the non-substituted acetylene ligand in $[3b]^+$ (Table 1).

2.1.2. Reaction of $(\eta^5\text{-C}_5\text{H}_4\text{Me})_4\text{Fe}_4(\text{HCCH})_2$ (**1**) with other reagents for bromination

The reaction of **1** with a mild bromination reagent BrCCl_3 in dichloromethane- d_2 was monitored by NMR spectroscopy. A mono-cationic form $[1]^+$ was formed instantaneously, but further reaction did not occur (Scheme 3).



Scheme 3.

The addition of excess Br_2 to a diethyl ether solution of **1**, followed by treatment with NH_4PF_6 , resulted in the formation of $[1](\text{PF}_6)_2$ in 75% yield (Scheme 3). In the reaction, Br_2 operated as a powerful oxidant to give the product through two-electron oxidation. No bromination of the acetylene ligands was observed. $[1](\text{PF}_6)_2$ was characterized by comparison with NMR data previously reported for $[1](\text{PF}_6)_2$ synthesized by the bulk electrolysis of **1** at 0.25 V vs. Ag/AgNO_3 $[3b]$. Once the dicationic species $[1]^{2+}$ was formed, bromination of the acetylene ligands did not proceed.

A solution containing **1** and 1 equiv. of Br_2 was prepared using the 1,4-dioxane adduct $\text{Br}_2 \cdot \text{C}_4\text{H}_8\text{O}_2$ as a bromination reagent. Treatment of **1** with 1 equiv. of $\text{Br}_2 \cdot \text{C}_4\text{H}_8\text{O}_2$ in dichloromethane at room temperature resulted in a mixture of $[2]^+$ and $[3a]^+$ in a molar ratio of 5:1 together with $[1]^{2+}$ (Scheme 3). Purification of these products was not successful. In the reaction of **1** with excess $\text{Br}_2 \cdot \text{C}_4\text{H}_8\text{O}_2$, $[1](\text{Br}_3)_2$ was formed exclusively and isolated in 79% yield (Scheme 3). Although the reaction of **1** with 1 equiv. of $\text{Br}_2 \cdot \text{C}_4\text{H}_8\text{O}_2$ resulted in partial bromination of the acetylene ligands, the poor selectivity of the reaction renders $\text{Br}_2 \cdot \text{C}_4\text{H}_8\text{O}_2$ unsuitable for bromination of the acetylenic protons in **1**.

2.2. X-ray diffraction analysis of $[2](\text{PF}_6)$, $[4](\text{TFPB})$, and $[5](\text{TFPB})$

Single crystals of $[4]^+$ and $[5]^+$ for X-ray diffraction analysis were prepared by replacing the counter anion with TFPB. The molecular structures of $[2](\text{PF}_6)$, $[4](\text{TFPB})$, and $[5](\text{TFPB})$ are illustrated in Figs. 1–3 and the interatomic distances and angles are listed in Tables 2–4. The asymmetric unit of $[2](\text{PF}_6)$ includes two independent molecules with no major differences between the two (only one is illustrated in Fig. 1). In cluster $[5](\text{TFPB})$, the atoms with asterisks are generated

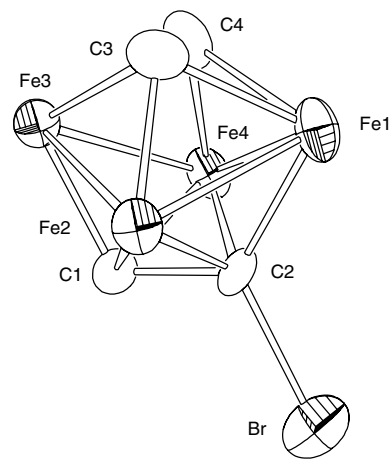


Fig. 1. Molecular structure of $[2](\text{PF}_6)$ at the 50% probability level. The counter anion and the $\eta^5\text{-C}_5\text{H}_4\text{Me}$ ligands are omitted for clarity.

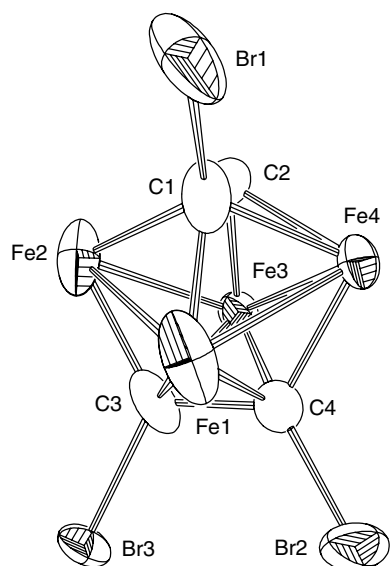


Fig. 2. Molecular structure of **[4](TFPB)** at the 50% probability level. The counter anion and the $\eta^5\text{-C}_5\text{H}_4\text{Me}$ ligands are omitted for clarity.

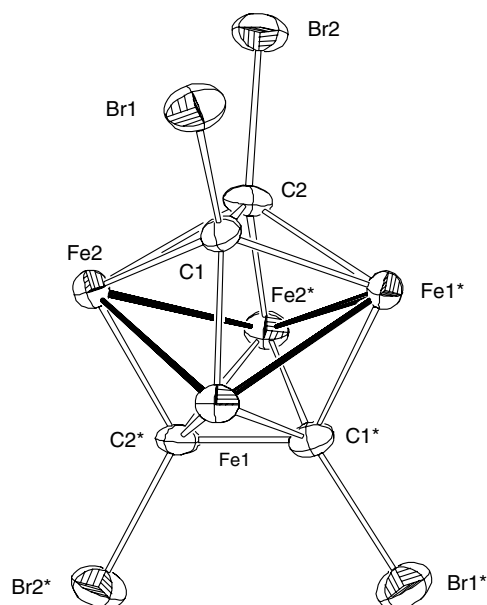


Fig. 3. Molecular structure of **[5](TFPB)** at the 50% probability level. The counter anion and the $\eta^5\text{-C}_5\text{H}_4\text{Me}$ ligands are omitted for clarity. Asterisks indicate atoms generated by the symmetry operation $(-x, y, 1/2-z)$.

by the symmetry operation $(-x, y, 1/2-z)$. The counter anions and the $\eta^5\text{-C}_5\text{H}_4\text{Me}$ ligands are omitted for clarity. In all clusters, the structural parameters around the Fe_4C_4 cores fall in the range observed for $[(\eta^5\text{-C}_5\text{H}_4\text{Me})_4\text{Fe}_4(\text{HCCH})_2](\text{TFPB})$ **[3d]**. The interatomic distances of the four iron–iron atoms indicate the existence of the four iron–iron bonds and no interaction between the two pairs $[\text{Fe1}\cdots\text{Fe3}$ and $\text{Fe2}\cdots\text{Fe4}$ in **[2](PF₆)** and **[4](TFPB)**; $\text{Fe1}\cdots\text{Fe2}^*$ and $\text{Fe1}^*\cdots\text{Fe2}$ in **[5](TFPB)**]. The torsion angles of four iron atoms are $37.30(6)^\circ$

Table 2
Interatomic distances (Å) and angles ($^\circ$) and torsion angles ($^\circ$) in $[(\eta^5\text{-C}_5\text{H}_4\text{Me})_4\text{Fe}_4(\text{HCCH})(\text{HCCBr})](\text{PF}_6)$ (**[2](PF₆)**)

Distances			
Fe1–Fe2	2.4710(19)	Fe1–Fe4	2.4924(19)
Fe2–Fe3	2.4646(19)	Fe3–Fe4	2.4724(19)
Fe1 \cdots Fe3	3.2987(19)	Fe2 \cdots Fe4	3.2973(18)
Fe1–C1	1.904(9)	Fe1–C3	2.009(10)
Fe1–C4	2.044(11)	Fe2–C1	1.959(9)
Fe2–C2	2.027(8)	Fe2–C3	1.953(11)
Fe3–C2	1.939(9)	Fe3–C3	2.035(9)
Fe3–C4	2.011(9)	Fe4–C1	2.006(10)
Fe4–C2	2.006(8)	Fe4–C4	1.950(10)
Br–C1	2.003(9)		
C1–C2	1.471(11)	C3–C4	1.502(14)
Angles			
Fe1–Fe2–Fe3	83.88(6)	Fe2–Fe3–Fe4	83.81(6)
Fe3–Fe4–Fe1	83.27(6)	Fe4–Fe1–Fe2	83.26(6)
Torsion angles			
Fe1–Fe2–Fe3–Fe4	37.30(6)	C1–C2–C3–C4	87.6 (7)

Table 3
Interatomic distances (Å) and angles ($^\circ$) and torsion angles ($^\circ$) in $[(\eta^5\text{-C}_5\text{H}_4\text{Me})_4\text{Fe}_4(\text{HCCBr})(\text{BrCCBr})](\text{TFPB})$ (**[4](TFPB)**)

Distances			
Fe1–Fe2	2.484(2)	Fe1–Fe4	2.5208(17)
Fe2–Fe3	2.4666(16)	Fe3–Fe4	2.4937(14)
Fe1 \cdots Fe3	3.2948(17)	Fe2 \cdots Fe4	3.3094(15)
Fe1–C1	1.917(12)	Fe1–C3	1.995(9)
Fe1–C4	1.998(9)	Fe2–C1	2.005(8)
Fe2–C2	1.997(8)	Fe2–C3	1.932(10)
Fe3–C2	1.928(8)	Fe3–C3	1.982(8)
Fe3–C4	2.002(8)	Fe4–C1	1.976(9)
Fe4–C2	1.984(8)	Fe4–C4	1.957(8)
Br1–C1	1.893(10)	Br2–C4	1.882(9)
Br3–C3	1.980(9)		
C1–C2	1.474(14)	C3–C4	1.478(11)
Angles			
Fe1–Fe2–Fe3	83.45(6)	Fe2–Fe3–Fe4	83.70(5)
Fe3–Fe4–Fe1	82.15(5)	Fe4–Fe1–Fe2	82.79(6)
Torsion angles			
Fe1–Fe2–Fe3–Fe4	38.86(6)	Br2–C4–C3–Br3	0.5(10)
C1–C2–C3–C4	84.4(6)		

(Fe1–Fe2–Fe3–Fe4 in **[2](PF₆)**), $38.86(6)^\circ$ (Fe1–Fe2–Fe3–Fe4 in **[4](TFPB)**), and $39.35(5)^\circ$ ($\text{Fe1–Fe1}^*-\text{Fe2}^*-\text{Fe2}$ in **[5](TFPB)**), which are close to that ($38.27(6)^\circ$) in **[1](TFPB)**. Thus, the tetrairon core is best described as having a butterfly geometry without the hinge iron–iron bond. Three types of acetylene fragments (HCCH, HCCBr, or BrCCBr) bridge the Fe_4 butterfly core in $\mu_4\text{-}\eta^2\text{:}\eta^2\text{:}\eta^1\text{:}\eta^1$ fashion. The bond length between the two carbon atoms in the acetylene ligands is close to that of a typical carbon–carbon single bond in hydrocarbons (1.54 Å) [5], reflecting electron-donation from the C–C π -bonding orbitals to the Fe_4 core and back donation from the Fe_4 core to the empty C–C π^* -antibonding orbitals. Accordingly, the Br–C

Table 4

Interatomic distances (Å) and angles (°) and torsion angles (°) in $[(\eta^5\text{-C}_5\text{H}_4\text{Me})_4\text{Fe}_4(\text{BrCCBr})_2](\text{TFPB})$ (**[5]**)(TFPB))

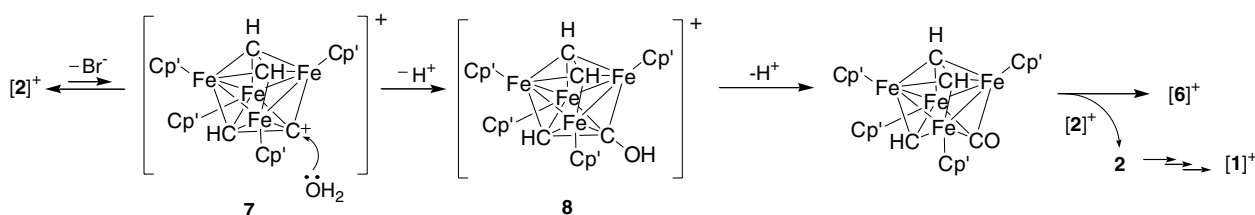
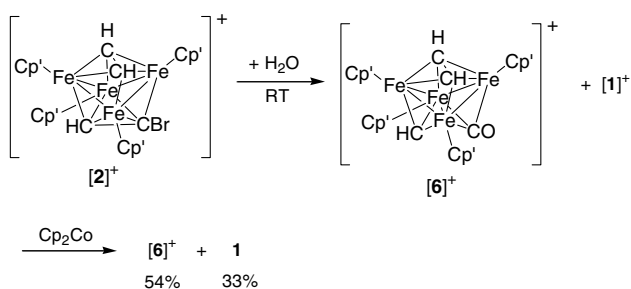
Distances			
Fe1–Fe2	2.510(1)	Fe1–Fe1*	2.472(2)
Fe2–Fe2*	2.475(2)	Fe1...Fe2*	3.296(1)
Fe1–C1	1.940(7)	Fe1–C1*	2.002(7)
Fe1–C2*	1.983(7)	Fe2–C1	1.979(7)
Fe2–C2	1.998(7)	Fe2–C2*	1.934(6)
Br1–C1	1.939(6)	Br2–C2	1.931(6)
C1–C2	1.49(1)		
Angles			
Fe1–Fe2–Fe2*	82.76(3)	Fe1*–Fe1–Fe2	82.83(3)
Torsion angles			
Fe1–Fe1*–Fe2*–Fe2	39.35(5)	C1–C2–C1*–C2*	82.9(7)
Br1–C1–C2–Br2	1.6(8)		

bond lengths in BrCCH and BrCCBr fragments (1.88–2.00 Å) lie in the range expected for bromoalkanes [C(sp³)–Br: 1.938(5) Å; –C=C–Br: 1.89(1) Å; Ar–Br: 1.85(1) Å; –C≡C–Br: 1.795(10) Å] **[5]**.

2.3. Reactivity of $[(\eta^5\text{-C}_5\text{H}_4\text{Me})_4\text{Fe}_4(\text{HCCH})(\text{HCCBr})]^{2+}$ (**[2]**)⁺ toward nucleophiles

2.3.1. Reaction of $[(\eta^5\text{-C}_5\text{H}_4\text{Me})_4\text{Fe}_4(\text{HCCH})(\text{HCCBr})]^{2+}$ (**[2]**)⁺ with water

X-ray diffraction analysis revealed that substitution of the acetylenic protons with bromine atoms did not affect the structure of the Fe₄C₄ core substantially. However, this is not the case for the reactivity. The cationic form **[1]**⁺ is entirely air-stable even in solution, in sharp contrast with **[2]**⁺. Reaction of **[2]**(PF₆) with water in



acetonitrile gave $[(\eta^5\text{-C}_5\text{H}_4\text{Me})_4\text{Fe}_4(\mu_3\text{-CO})(\mu_3\text{-CH})(\text{HCCH})](\text{PF}_6)$ (**[6]**(PF₆)) via cleavage of the carbon–carbon bond together with the minor formation of **[1]**(PF₆) (**Scheme 4**). The cyclic voltammograms of **[1]**(PF₆) and **[6]**(PF₆) displayed reversible one-electron reduction waves at $E_{1/2} = -0.73$ and -1.32 V vs. Ag/AgNO₃, respectively, indicating that **[1]**(PF₆) is more easily reduced than **[6]**(PF₆) **[4]**. After removal of volatiles, treatment of the residue with Cp₂Co resulted in one-electron reduction of **[1]**(PF₆), whereas **[6]**(PF₆) remained intact. Extraction of the residue with hexane and then dichloromethane, followed by evaporation of the two extracts, gave **[6]**(PF₆) and **1** in 54% and 33% isolated yields, respectively. Experiments using H₂¹⁸O and D₂O revealed that the oxygen atom of CO in **[6]**⁺ and one of the hydrogen atoms of HCCH in **[1]**⁺ are derived from water. The infrared (IR) spectrum of $[(\eta^5\text{-C}_5\text{H}_4\text{Me})_4\text{Fe}_4(\mu_3\text{-C}^{18}\text{O})(\mu_3\text{-CH})(\text{HCCH})]^{2+}$ includes a band at 1675 cm⁻¹ assignable to a terminal C–¹⁸O stretching vibration mode. The ²H NMR spectrum of $[(\eta^5\text{-C}_5\text{H}_4\text{Me})_4\text{Fe}_4(\text{HCCH})(\text{HCCD})]^{2+}$ displays a signal at $\delta = -76.3$ assignable to HCCD.

The formation of **[6]**(PF₆) may be most easily understood to occur via an S_N2-type mechanism to give the ethynol-coordinated cluster $[(\eta^5\text{-C}_5\text{H}_4\text{Me})_4\text{Fe}_4(\text{HCCH})(\text{HCC-OH})](\text{PF}_6)$ (**8**): The H₂O molecule attacks the electrophilic carbon atom of the HCCBr fragment from the side opposite the leaving bromo group. However, as it is unlikely to be a vacant site opposite the leaving bromo group, an alternative mechanism involving an S_N1-type process through the initial dissociation of the bromo group is tentatively proposed (**Scheme 5**). The resulting $[(\eta^5\text{-C}_5\text{H}_4\text{Me})_4\text{Fe}_4(\text{HCCH})(\text{HCC})]^{2+}$ (**7**) undergoes nucleophilic attack by water to give **8**. At this time there is no direct evidence available to distinguish between the two mechanisms. The isomerization of **8** to the keto-form, followed by deprotonation and oxidation, affords **[6]**(PF₆), in which **[2]**(PF₆) operates as an oxidant and is converted to **2**. Preliminary analysis of the electrochemistry of **[2]**(PF₆) revealed that the neutral cluster **2** does not exist as a stable form. The decomposition of **2** is thus thought to lead to the formation of **[1]**⁺.

Boyar et al. **[6]** reported the isomerization of an ethynol cluster Os₃H₂(μ₃-HCCOH)(CO)₉ to the corresponding keto-form Os₃H₃(μ₃-HCCO)(CO)₉, with the

resultant decarbonylation giving the methylidyne cluster $\text{Os}_3\text{H}_3(\mu_3\text{-CH})(\text{CO})_9$. Vollhardt and Wolfgruber [7] synthesized and structurally characterized an ethynol-coordinated tricobalt cluster $[\text{Cp}_3\text{Co}_3(\mu_3\text{-CH})(\mu_3\text{-HC-COH})]^+$, which caused decarbonylation and coupling of two methylidyne ligands to give $[\text{Cp}_3\text{Co}_3(\mu\text{-H})(\mu\text{-CO})(\mu_3\text{-HCCH})]^+$. It should be noted that haloalkynes are considerably stable toward water [1]. Thus, the reactivity discovered here is characteristic of the bromoacetylene fragment coordinated to the tetrairon core.

It has been known that even in the neutral σ,π -ethynyl complex, the α -carbon shows the carbocationic reactivity: the σ,π -ethynyl complexes react with nucleophiles to give the zwitterionic adducts [8]. In cluster **7** generated in situ, the cationic ethynyl fragment would exhibit the enhanced reactivity toward nucleophiles, leading to rich reactivity.

2.3.2. Reaction of $[(\eta^5\text{-C}_5\text{H}_4\text{Me})_4\text{Fe}_4(\text{HCCH})\text{-}(\text{HCCBr})^+]$ (**[2]**⁺) with ZnR_2 ($\text{R} = \text{Me}, \text{Et}$), HCCMgBr , and LiS^pTol

Treatment of **[2]**(TFPB) with ZnR_2 ($\text{R} = \text{Me}, \text{Et}$) in diethyl ether at room temperature led to elongation of the carbon–carbon chain to give **[9]**(TFPB) (88%) and **[10]**(TFPB) (91%) (Scheme 6). The reaction of **[2]**(TFPB) with $\text{H-C}\equiv\text{CMgBr}$ in diethyl ether at room temperature gave **[11]**(TFPB) in 95% yield, and the reaction of **[2]**(PF₆) with LiS^pTol in acetonitrile at room temperature gave **[12]**(PF₆) in 78% yield. These products were isolated by the appropriated methods (see Section 4) and have been characterized by elemental analysis and NMR spectroscopy (Table 1). In the ¹H NMR spectra of **[9]**(TFPB), **[10]**(TFPB), and **[11]**(TFPB), the signals

of the incorporated CH_3 , CH_2CH_3 , and $\text{C}\equiv\text{CH}$ groups appear at δ -27.5 (CH_3), -37.1 (CH_2CH_3) and -4.6 (CH_2CH_3), and 10.31 ($\text{C}\equiv\text{CH}$), respectively. The signals of the S^pTol group in **[12]**(PF₆) appear at δ 1.39 ($\text{SC}_6\text{H}_4\text{CH}_3$) 5.10, and 6.35 ($\text{SC}_6\text{H}_4\text{CH}_3$).

Clusters **[9]**(BPh₄) and **[12]**(PF₆) were further characterized by X-ray diffraction analysis. The molecular structures of the cationic parts in **[9]**(BPh₄) and **[12]**(PF₆) are illustrated in Figs. 4 and 5, and selected interatomic distances and angles are listed in Tables 5 and 6. Both clusters have an Fe₄ butterfly arrangement

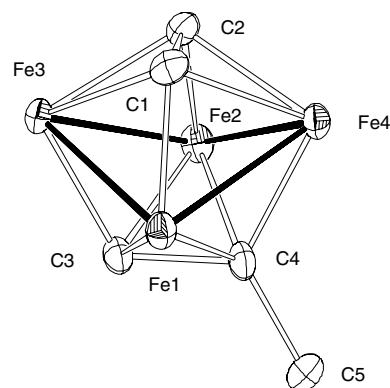


Fig. 4. Molecular structure of **[9]**(BPh₄) at the 50% probability level. The counter anion and the $\eta^5\text{-C}_5\text{H}_4\text{Me}$ ligands are omitted for clarity.

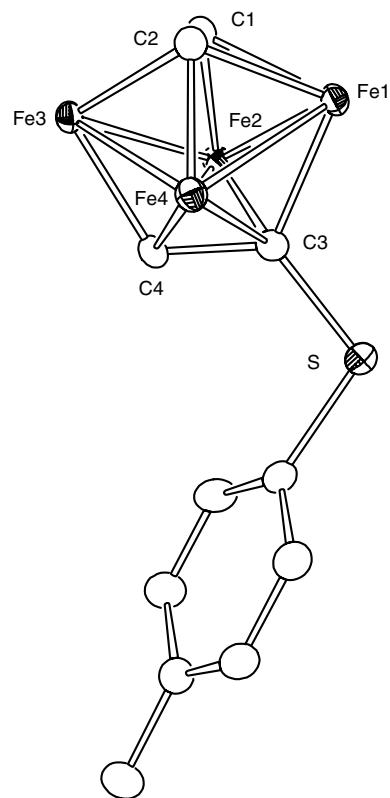
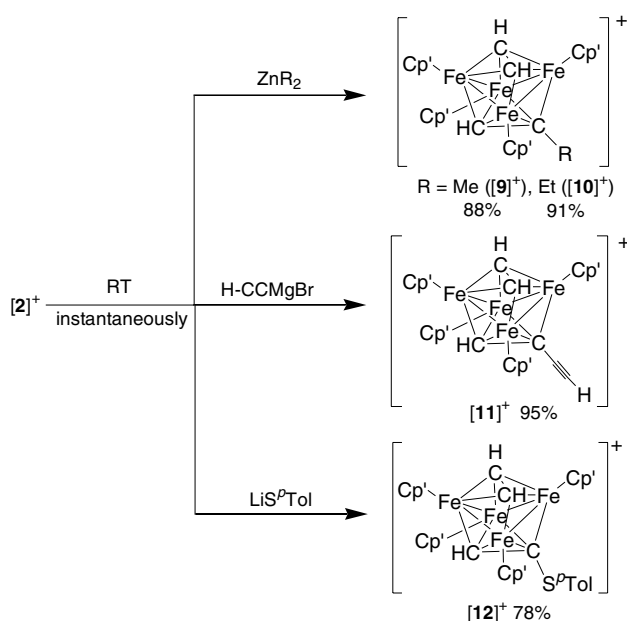


Fig. 5. Molecular structure of **[12]**(PF₆) at the 50% probability level. The counter anion and the $\eta^5\text{-C}_5\text{H}_4\text{Me}$ ligands are omitted for clarity.



Scheme 6.

Table 5

Interatomic distances (Å) and angles (°) and torsion angles (°) in $[(\eta^5\text{-C}_5\text{H}_4\text{Me})_4\text{Fe}_4(\text{HCCH})(\text{HCC-Me})(\text{BPh}_4)]$ (**[9]**(BPh₄))

Distances			
Fe1–Fe3	2.450(1)	Fe1–Fe4	2.475(1)
Fe2–Fe3	2.480(1)	Fe2–Fe4	2.447(1)
Fe1···Fe2	3.276(1)	Fe3···Fe4	3.275(1)
Fe1–C1	1.934(7)	Fe1–C3	2.008(6)
Fe1–C4	1.981(7)	Fe2–C2	1.917(6)
Fe2–C3	1.985(7)	Fe2–C4	2.025(7)
Fe3–C1	2.004(7)	Fe3–C2	1.990(7)
Fe3–C3	1.929(6)	Fe4–C1	1.992(6)
Fe4–C2	2.002(6)	Fe4–C4	1.953(7)
C1–C2	1.489(9)	C3–C4	1.472(8)
C4–C5	1.534(9)		
Angles			
Fe1–Fe3–Fe2	83.29(4)	Fe3–Fe2–Fe4	83.30(4)
Fe2–Fe4–Fe1	83.45(4)	Fe4–Fe1–Fe3	83.36(4)
Torsion angles			
Fe1–Fe3–Fe2–Fe4	37.81(4)	C1–C2–C3–C4	83.2(5)

Table 6

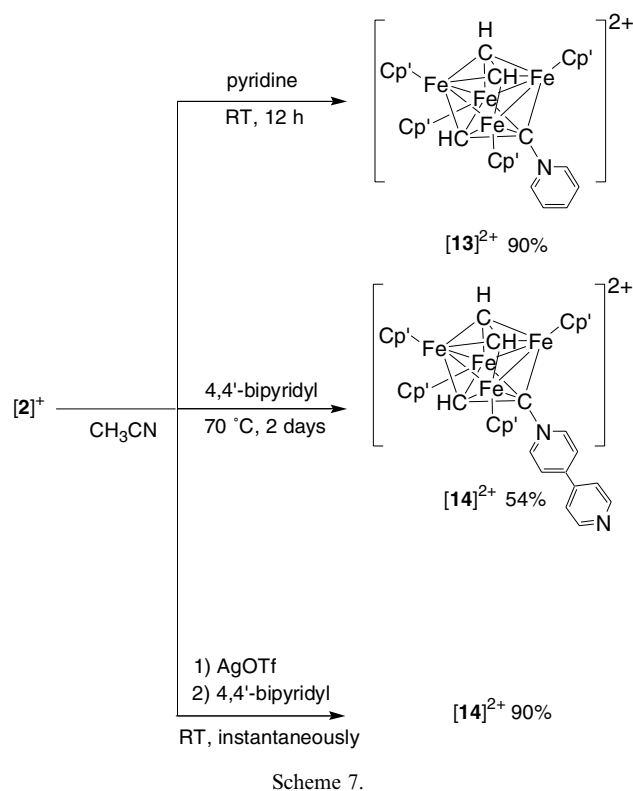
Interatomic distances (Å) and angles (°) and torsion angles (°) in $[(\eta^5\text{-C}_5\text{H}_4\text{Me})_4\text{Fe}_4(\text{HCCH})(\text{HCC-S}^p\text{Tol})(\text{PF}_6)]$ (**[12]**(PF₆))

Distances			
Fe1–Fe2	2.4760(4)	Fe1–Fe4	2.5003(4)
Fe2–Fe3	2.4599(4)	Fe3–Fe4	2.4527(4)
Fe1···Fe3	3.2684(4)	Fe2···Fe4	3.3072(4)
Fe1–C1	1.990(2)	Fe1–C2	1.990(2)
Fe1–C3	1.953(2)	Fe2–C1	1.935(2)
Fe2–C3	2.041(2)	Fe2–C4	2.010(2)
Fe3–C1	1.987(2)	Fe3–C2	1.996(2)
Fe3–C4	1.949(2)	Fe4–C2	1.928(2)
Fe4–C3	2.025(2)	Fe4–C4	2.001(2)
S–C3	1.783(2)		
C1–C2	1.484(3)	C3–C4	1.477(3)
Angles			
Fe1–Fe2–Fe3	82.931(13)	Fe2–Fe3–Fe4	84.628(14)
Fe3–Fe4–Fe1	82.575(14)	Fe4–Fe1–Fe2	83.298(13)
Torsion angles			
Fe1–Fe2–Fe3–Fe4	38.00 (1)	C1–C2–C3–C4	84.86(16)

without the hinge metal–metal bond very similar to non-substituted bis(acetylene) cluster **[1]**(TFPB), and the bond lengths and angles are also comparable to the corresponding features in **[1]**(TFPB). In **[9]**(BPh₄) and **[12]**(PF₆), the bromine group is displaced by methyl and toluene thiolate groups, respectively. The bond distances for C4–C5 (1.534(9) Å) and S–C3 (1.783(2) Å) are in the normal range expected for each single bond [5].

2.3.3. Reactions of $[(\eta^5\text{-C}_5\text{H}_4\text{Me})_4\text{Fe}_4(\text{HCCH})(\text{HCCBr})]^+$ (**[2]**)⁺ with pyridine and 4,4'-bipyridyl

The bromo group on the acetylene was easily substituted with pyridine by treatment at room temperature for 12 h to give **[13]**(PF₆)₂ in 90% yield (Scheme 7). Substitution with 4,4'-bipyridyl (bpy) requires more severe conditions (70 °C, 2 days), giving the product **[14]**(PF₆)₂



in only 54% yield. The poor reactivity toward bpy is attributable to its relative low basicity ($\text{p}K_{\text{a}1} = 3.17$, $\text{p}K_{\text{a}2} = 4.82$) compared to pyridine ($\text{p}K_{\text{a}} = 5.17$) [5]. Addition of silver salt to the solution of **[2]**(PF₆) and bpy led to abstraction of the bromo group to give **[14]**(PF₆)₂ instantaneously in 90% yield.

Clusters **[13]**(PF₆)₂ and **[14]**(PF₆)₂ were characterized by elemental analysis and spectroscopy, and the molecular structure of **[13]**(PF₆)₂ was established by X-ray diffraction analysis (Fig. 6). The interatomic distances and angles are listed in Table 7. The structure of the Fe₄C₄ core is essentially the same as that in **[1]**(TFPB), and the N–C1 bond distance (1.492(9) Å) lies in the normal range expected for the pyridinium–carbon bonds [9]. Boyar et al. [6] reported the synthesis of Os₃H(μ₃-HCCPy)(CO)₉, which is a rare example of a pyridinium-substituted acetylene cluster. However, to our best knowledge, cluster **[13]**(PF₆)₂ is the first example of this type to be characterized by X-ray diffraction analysis.

As proposed for the mechanism of the reaction of **[2]**⁺ with water (Scheme 5), the formation of **[13]**²⁺ and **[14]**²⁺ can be explained as due to the transient formation of the ethynyl cation-coordinated cluster **7** via dissociation of the bromo group, which is in fast equilibrium with **[2]**⁺. Intermediate **7** undergoes nucleophilic attack by pyridines to give the products. Treatment with silver salt shifts the equilibrium to the right through abstraction of the bromo group and enhances the formation of **[14]**(PF₆)₂.

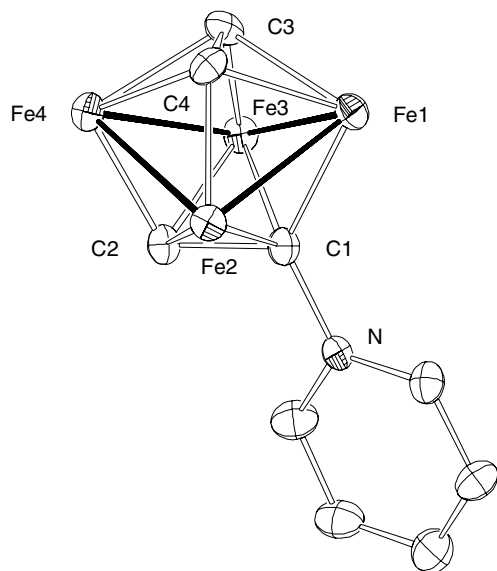


Fig. 6. Molecular structure of $[\mathbf{13}](\text{PF}_6)_2 \cdot 1/2\text{CH}_3\text{CN}$ at the 50% probability level. The counter anion, the solvated acetonitrile, and the $\eta^5\text{-C}_5\text{H}_4\text{Me}$ ligands are omitted for clarity.

Table 7

Interatomic distances (Å) and angles ($^\circ$) and torsion angles ($^\circ$) in $[(\eta^5\text{-C}_5\text{H}_4\text{Me})_4\text{Fe}_4(\text{HCCH})(\text{HCC-Py})](\text{PF}_6)_2$ ($[\mathbf{13}](\text{PF}_6)_2$)

Distances			
Fe1–Fe2	2.4844(14)	Fe1–Fe3	2.4530(15)
Fe2–Fe4	2.4903(15)	Fe3–Fe4	2.5024(15)
Fe1···Fe4	3.2869(15)	Fe2···Fe3	3.2891(15)
Fe1–C1	1.995(7)	Fe1–C3	1.991(8)
Fe1–C4	1.984(7)	Fe2–C1	1.987(7)
Fe2–C2	2.030(8)	Fe2–C4	1.938(7)
Fe3–C1	1.988(7)	Fe3–C2	2.013(7)
Fe3–C3	1.942(8)	Fe4–C2	1.919(7)
Fe4–C3	1.984(8)	Fe4–C4	1.993(8)
N–C1	1.492(9)		
C1–C2	1.491(10)	C3–C4	1.470(11)
Angles			
Fe1–Fe2–Fe4	82.71(5)	Fe1–Fe3–Fe4	83.10(5)
Fe3–Fe1–Fe2	83.54(5)	Fe2–Fe4–Fe3	82.42(5)
Torsion angles			
Fe1–Fe2–Fe4–Fe3	38.16(4)	C1–C2–C3–C4	84.4 (5)

3. Summary

Using various amounts of NBS as a bromination reagent, $[(\eta^5\text{-C}_5\text{H}_4\text{Me})_4\text{Fe}_4(\text{HCCH})(\text{HCCBr})](\text{OTf})$, $[(\eta^5\text{-C}_5\text{H}_4\text{Me})_4\text{Fe}_4(\text{HCCBr})_2](\text{OTf})$, $[(\eta^5\text{-C}_5\text{H}_4\text{Me})_4\text{Fe}_4(\text{HCCBr})(\text{BrCCBr})](\text{OTf})$, and $[(\eta^5\text{-C}_5\text{H}_4\text{Me})_4\text{Fe}_4(\text{BrC-$

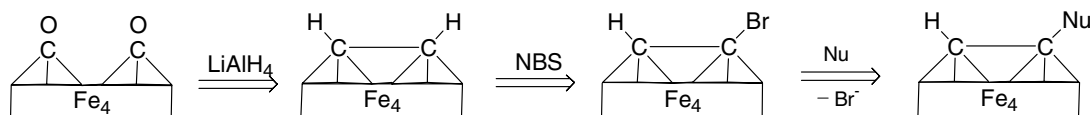
$\text{CBr})_2](\text{OTf})$ were synthesized in good yields. In the reactions of $\mathbf{1}$ with Br_2 or excess $\text{Br}_2 \cdot \text{C}_4\text{H}_8\text{O}_2$, the dicationic form $[\mathbf{1}]^{2+}$ was formed exclusively and no further bromination of the acetylene ligands occurred. Reaction with 1 equiv. of $\text{Br}_2 \cdot \text{C}_4\text{H}_8\text{O}_2$ led to the formation of $[\mathbf{2}]^+$ and $[\mathbf{3a}]^+$ together with $[\mathbf{1}]^{2+}$, although with lower selectivity and yield.

In organic syntheses, alkyne derivatives can be easily synthesized by reactions between anionic acetylide compounds and a variety of electrophiles. On the butterfly type tetrairon core, the acetylene fragment can be functionalized by the reaction with bromoacetylene, which can be regarded as synthon for the unprecedented *cationic ethynyl fragment* (HCC^+) through dissociation of the bromo group, with *nucleophiles*. Thus, two carbon monoxide molecules are totally converted to the functionalized alkyne fragments through the formation of acetylene $[\mathbf{3a}]$ and bromoacetylene on the tetrairon clusters, as illustrated in Scheme 8.

The Fe_4C_4 cluster $\mathbf{1}$ exhibits three reversible one-electron oxidation waves ($E_{1/2} = -0.73, +0.17, +0.96$ V vs Ag/AgNO_3) and an irreversible one-electron reduction wave ($E_{\text{pc}} = -1.38$ V) $[\mathbf{3a}]$. Taking account of the low $E_{1/2}$ values, $\mathbf{1}$ may represent an efficient multi-electron donor. Using the candidates $[\mathbf{11}]^+$ and $[\mathbf{14}]^{2+}$, having the ethynyl and 4,4'-bipyridyl groups on the acetylene ligands, the electron-rich Fe_4C_4 core can be bonded with itself, other functional transition-metal complexes, and organic compounds through the π -conjugated linkers $[\mathbf{10}, \mathbf{11}]$. The properties of the resulting giant molecules can be expected to be of great interest, and are currently under investigation.

4. Experimental

All manipulations were carried out under dry nitrogen or vacuum using standard Schlenk techniques or in a nitrogen-filled glovebox. Reagent-grade diethyl ether and hexane were distilled from sodium-benzophenone immediately prior to use. Acetonitrile and dichloromethane were distilled from CaH_2 . Dichloromethane- d_2 and acetonitrile- d_3 were distilled from CaH_2 and further dried over 4A molecular sieves. The compounds $(\eta^5\text{-C}_5\text{H}_4\text{Me})_4\text{Fe}_4(\text{CO})_4$ $[\mathbf{12}]$ and Cp_2Co $[\mathbf{13}]$ were prepared according to published procedures. All other chemicals were used as received. NMR spectra were recorded on a Bruker ARX-300 or AV-300 spectrometer. ^1H NMR chemical shifts are reported relative to SiMe_4 and were



Scheme 8.

determined by references to the residual ^1H solvent resonances. IR spectra were recorded on a Horiba FT-200 spectrometer. Mass spectral data were obtained using a JEOL JMS-HX110. Cyclic voltammetry was carried out with a Bioanalytical System BAS-100BW electrochemical analyzer. Measurements were made in 0.1 mol dm^{-3} tetrabutylammonium tetrafluoroborate (TBAB)/acetonitrile solutions with a three electrode system with a Pt rod working electrode, a Pt coil auxiliary electrode, and an Ag/AgNO₃ reference electrode.

4.1. Reaction of $(\eta^5\text{-C}_5\text{H}_4\text{Me})_4\text{Fe}_4(\text{HCCH})_2$ (**1**) with 1 equiv. of *N*-bromosuccinimide (NBS)

NBS (13 mg, 0.073 mmol) was added to a dichloromethane solution (5 mL) of **1** [**3b**] (50 mg, 0.085 mmol) at room temperature. The color of the solution immediately changed from brown to greenish brown. After stirring the solution for 15 min, volatiles were removed under reduced pressure. Recrystallization of the residue from acetonitrile/diethyl ether at 0°C gave a brown solid of [**1**]Br. Yield: 47 mg (83%). Anal. calc. for $\text{C}_{28}\text{H}_{32}\text{BrFe}_4$: C, 50.06; H, 4.80. Found: C, 49.78, H, 4.83%. IR (KBr, cm^{-1}) 2964 (w), 2933 (w), 1654 (w), 1637 (w), 1448 (w), 1261 (m), 1160 (w), 1110 (m), 1027 (m), 800 (m), 669 (m). ^1H NMR (300 MHz, CD_3CN) δ -75.2 (br, $W_{1/2} = 53 \text{ Hz}$, 4H, 2HCCH), -1.4 (br, $W_{1/2} = 7.8 \text{ Hz}$, 12H, $\text{C}_5\text{H}_4\text{Me}$), 6.0, 8.9 (br, $W_{1/2} = 18 \text{ Hz}$, 8H $\times 2$, $\text{C}_5\text{H}_4\text{Me}$). $^{13}\text{C}\{^1\text{H}\}$ NMR (75.5 MHz, CD_3CN): δ 13.1 ($\text{C}_5\text{H}_4\text{Me}$), 93.0, 105.2, 121.3 ($\text{C}_5\text{H}_4\text{Me}$). ^{13}C NMR signals of HCCH were not assigned.

4.2. Reaction of [**1**](OTf) with 1 equiv. of NBS

To a dichloromethane solution (10 mL) of [**1**](OTf) (204 mg, 0.275 mmol) was added NBS (49 mg, 0.28 mmol) at room temperature. After stirring the reaction mixture for 30 min, volatiles were removed under reduced pressure. The greenish brown residue was extracted with diethyl ether. Evaporation of the extract under reduced pressure gave succinimide (23 mg, 82%). The insoluble material was extracted with dichloromethane and the extract was concentrated to dryness under reduced pressure to give a greenish brown solid of $[(\eta^5\text{-C}_5\text{H}_4\text{Me})_4\text{Fe}_4(\text{HCCH})(\text{HCCBr})](\text{OTf})$ (**[2](OTf)**). Yield: 204 mg (91%). Anal. calc. for $\text{C}_{29}\text{H}_{31}\text{BrF}_3\text{Fe}_4\text{O}_3\text{S}$: C, 42.48; H, 3.81. Found: C, 42.01; H, 4.07%. Mass (FAB) m/z 671 ($\text{M}^+ - \text{OTf}$, 60), 591 ($\text{M}^+ - \text{OTf} - \text{Br}$, 79). IR (KBr, cm^{-1}) 3102 (w), 3091 (w), 2923 (w), 2852 (w), 1479 (m), 1457 (m), 1371 (m), 1265 (vs, ν (S-O)), 1220 (m), 1145(m), 1027 (s), 825 (m), 723(m), 636 (vs), 593 (m), 514 (m). ^1H NMR (300 MHz, CD_3CN) δ -70.6 (br, $W_{1/2} = 50 \text{ Hz}$, 2H, HCCH), -61.0 (br, $W_{1/2} = 42 \text{ Hz}$, 1H, HCCBr), -6.5, -2.7 (br, $W_{1/2} = 15 \text{ Hz}$, 3H $\times 2$, $\text{C}_5\text{H}_4\text{Me}$), 0.01 (br, $W_{1/2} = 15 \text{ Hz}$, 6H,

$\text{C}_5\text{H}_4\text{Me}$), 3.9, 4.2, 5.8, 7.5, 8.7, 9.4, 10.7, 11.2 (br, $W_{1/2} = 24 \text{ Hz}$, 2H $\times 8$, $4\text{C}_5\text{H}_4\text{Me}$). $^{13}\text{C}\{^1\text{H}\}$ NMR (75.5 MHz, CD_3CN) δ 8.9, 17.6, 23.8 ($\text{C}_5\text{H}_4\text{Me}$), 75.1, 80.8, 92.4, 98.7, 106.7, 116.1, 123.5, 127.3, 127.5, 128.8, 134.8 ($\text{C}_5\text{H}_4\text{Me}$). ^{13}C NMR signals of HCCH and HCCBr were not assigned.

[2](PF₆) and **[2](TFPB)** were obtained by similar methods, using [**1**](PF₆) (308 mg, 0.418 mmol) and NBS (74 mg, 0.42 mmol) and [**1**](TFPB) (1.83 g, 1.26 mmol) and NBS (229 mg, 1.29 mmol), respectively. Yield of **[2](PF₆)**: 326 mg (96%). Anal. calc. for $\text{C}_{28}\text{H}_{31}\text{BrF}_6\text{Fe}_4\text{P}$: C, 41.22; H, 3.83. Found: C, 40.82; H, 3.82%. Yield of **[2](TFPB)**: 1.61 g (83%). Anal. calc. for $\text{C}_{60}\text{H}_{43}\text{BBBrF}_{24}\text{Fe}_4$: C, 46.98; H, 2.83. Found: C, 46.87; H, 3.02%.

4.3. Reaction of [**2**](OTf) with 1 equiv. of NBS

A dichloromethane solution (20 mL) of [**2**](OTf) (102 mg, 0.124 mmol) was treated with NBS (22 mg, 0.12 mmol) at room temperature. After stirring the solution at room temperature for 2 h, the mixture was concentrated to dryness under reduced pressure. The greenish brown residue was washed with diethyl ether and then extracted with dichloromethane. The solvent was removed from the extract under reduced pressure to give a greenish brown solid of $[(\eta^5\text{-C}_5\text{H}_4\text{Me})_4\text{Fe}_4(\text{HCCBr})_2](\text{OTf})$ (**[3a](OTf)**). Yield: 80 mg (72%). Anal. calc. for $\text{C}_{29}\text{H}_{30}\text{Br}_2\text{F}_3\text{Fe}_4\text{O}_3\text{S}$: C, 38.75; H, 3.36. Found: C, 39.26; H, 3.53%. Mass (FAB) m/z 749 ($\text{M}^+ - \text{OTf}$, 66), 669 ($\text{M}^+ - \text{OTf} - \text{Br}$, 40), 591 ($\text{M}^+ - \text{OTf} - 2\text{Br}$, 28). IR (KBr, cm^{-1}): 3102 (w), 3095 (w), 2958 (w), 2923 (w), 2852 (w), 1481 (m), 1450 (m), 1371 (m), 1265 (vs, ν_{SO}), 1222 (m), 1147(m), 1027 (s), 825 (m), 723(m), 636 (vs), 593 (m). ^1H NMR (300 MHz, CD_3CN) δ -57.2 (br, $W_{1/2} = 42 \text{ Hz}$, 2H, HCCBr), -5.4, -1.2 (br, $W_{1/2} = 12 \text{ Hz}$, 6H $\times 2$, $\text{C}_5\text{H}_4\text{Me}$), 1.0, 4.1, 7.1, 9.6, 10.2, 11.0 (br, $W_{1/2} = 27 \text{ Hz}$, 2H $\times 6$, $\text{C}_5\text{H}_4\text{Me}$), 10.9 (br, 2H $\times 2$, accidentally overlapped, $\text{C}_5\text{H}_4\text{Me}$). $^{13}\text{C}\{^1\text{H}\}$ NMR (75.5 MHz, CD_3CN): δ 13.1, 19.7 ($\text{C}_5\text{H}_4\text{Me}$), 63.3, 77.6, 86.8, 105.4, 111.2, 122.2, 126.4, 130.8, 136.9, 161.2 ($\text{C}_5\text{H}_4\text{Me}$). ^{13}C NMR signals of HCCBr were not assigned.

4.4. Monitoring of reaction of [**2**](OTf) with 1 equiv. of NBS

A Pyrex NMR tube (5 mm o.d.) was charged with [**2**](OTf) (20 mg, 0.024 mmol), NBS (5 mg, 0.03 mmol), and CD_2Cl_2 (0.5 mL) in a glovebox. The tube was connected to a vacuum line and flame-sealed under reduced pressure. The reaction was monitored at room temperature by ^1H NMR spectroscopy. [**2**](OTf) was consumed within 30 min, and **[3a](OTf)** and $[(\eta^5\text{-C}_5\text{H}_4\text{Me})_4\text{Fe}_4(\text{HCCH})(\text{BrCCBr})](\text{OTf})$ (**[3b](OTf)**) were formed in a 3:1 molar ratio. ^1H NMR for **[3b](OTf)** (300

MHz, CD₃CN) δ -67.4 (br, 2H, HCCH), -7.0, 1.1 (br, Hz, 6H \times 2, C₅H₄Me), 3.7, 7.7, 8.1, 12.1 (br, 2H \times 4, C₅H₄Me).

4.5. Reaction of [3a](OTf) with 1.4 equiv. of NBS

A dichloromethane solution (15 mL) of [3a](OTf) (110 mg, 0.122 mmol) was treated with NBS (31 mg, 0.17 mmol) at room temperature. After stirring the solution at room temperature for 8 h, the mixture was concentrated to dryness under reduced pressure. The greenish brown residue was washed with diethyl ether and then extracted with dichloromethane. The solvent was removed from the extract to give a greenish brown solid of $[(\eta^5\text{-C}_5\text{H}_4\text{Me})_4\text{Fe}_4(\text{HCCBr})(\text{BrCCBr})](\text{OTf})$ ([4](OTf)). Yield: 89 mg (75%). Anal. calc. for C₂₉H₂₉Br₃F₃Fe₄O₃S: C, 35.63; H, 2.99. Found: C, 35.70; H, 3.12%. Mass (ESI) *m/z* 828 (M⁺ - OTf), 765 (M⁺ - SO₂CF₃ - Br), 750 (M⁺ - OTf - Br). IR (KBr, cm⁻¹): 3102 (w), 3095 (w), 2958 (w), 2921 (w), 2852 (w), 1481 (m), 1457 (m), 1369 (m), 1265 (vs, ν_{SO}), 1222 (m), 1151 (m), 1027 (s), 858 (w), 835 (m), 792 (w), 730 (m), 636 (vs), 570 (w), 514 (w). ¹H NMR (300 MHz, CD₃CN): δ -54.0 (br, $W_{1/2}$ = 47 Hz, 1H, HCCBr), -6.0 (br, $W_{1/2}$ = 10 Hz, 6H, 2C₅H₄Me), -5.6, 0.2 (br, $W_{1/2}$ = 10 Hz, 3H \times 2, 2C₅H₄Me), -0.9, 7.2, 9.6, 10.8, 11.1, 11.8 (br, $W_{1/2}$ = 24 Hz, 2H \times 6, 4C₅H₄Me), 7.9 (br, 2H \times 2, accidentally overlapped, C₅H₄Me). ¹³C{¹H} NMR (75.5 MHz, CD₃CN): δ 10.2, 18.4, 19.1 (C₅H₄Me), 61.9, 98.1, 99.8, 101.1, 105.6, 110.9, 123.5, 124.1, 130.3, 147.7, 157.0 (C₅H₄Me). ¹³C NMR signals of HCCBr and BrCCBr were not assigned.

4.6. Reaction of [4](OTf) with NBS

A Pyrex NMR tube (5 mm o.d.) was charged with [4](OTf) (20 mg, 0.021 mmol), NBS (4 mg, 0.02 mmol), and CD₂Cl₂ (0.5 mL) in a glovebox. The tube was connected to a vacuum line and flame-sealed. The reaction was monitored at room temperature by ¹H NMR spectroscopy. After 3 days, the molar ratio of [4](OTf) and $[(\eta^5\text{-C}_5\text{H}_4\text{Me})_4\text{Fe}_4(\text{BrCCBr})_2](\text{OTf})$ ([5](OTf)) was 1:1. The NMR tube was opened in the glovebox, and NBS (8 mg, 0.04 mmol) was added to the reaction mixture. After complete consumption of [4](OTf), taking 4 days in total, volatiles were removed under reduced pressure and the residue was washed with diethyl ether to remove succinimide. The insoluble material was extracted with dichloromethane and the extract was filtered through a Celite pad. The filtrate was evaporated to dryness to give [5](OTf). Yield: 15 mg (69%). Anal. calc. for C₂₉H₂₈Br₄F₃Fe₄O₃S: C, 32.97; H, 2.67. Found: C, 32.85; H, 2.89%. Mass (FAB) *m/z* 908 (M⁺ - OTf, 91), 828 (M⁺ - OTf - Br, 30), 748 (M⁺ - OTf - 2Br, 16), 669 (M⁺ - OTf - 3Br, 14). IR (KBr, cm⁻¹): 3091 (w), 2964 (w), 2919 (w), 2852 (w), 1369 (w), 1268 (vs, ν_{SO}),

1147(s), 1027 (s), 863 (m), 794 (w), 636 (s). ¹H NMR (300 MHz, CD₃CN): δ -5.5 (br, $W_{1/2}$ = 14 Hz, 12H, 4C₅H₄Me), 6.8, 10.0 (br, $W_{1/2}$ = 24 Hz, 8H \times 2, 4C₅H₄Me). ¹³C{¹H} NMR (75.5 MHz, CD₃CN): δ 19.2 (C₅H₄Me), 104.4, 126.6, 128.7 (C₅H₄Me). ¹³C NMR signal of BrCCBr was not assigned.

4.7. Reaction of 1 with Br₂

To a solution of 1 (150 mg, 0.253 mg) in CH₂Cl₂ (20 mL) was added Br₂ (404 mg, 2.53 mmol) at room temperature. The dark green precipitates were separated by filtration and washed with diethyl ether. The solid was dissolved in water and was treated with NH₄PF₆ (500 mg, 3.07 mmol). The dark green precipitates were formed again and separated by filtration and washed with water and diethyl ether, then extracted with acetonitrile. Removal of the solvent from the extract gave a brown solid of [1](PF₆)₂. Yield: 168 mg (75%).

4.8. Reaction of 1 with 1 equiv. Br₂ · C₄H₈O₂

To a solution of 1 (50 mg, 0.085 mmol) in CH₂Cl₂ (5 mL) was added Br₂ · C₄H₈O₂ (21 mg, 0.085 mmol) at room temperature under constant stirring. The resultant greenish brown suspension was filtered through a Celite pad and the insoluble material was extracted with CH₂Cl₂ (5 mL \times 2) and then acetonitrile (20 mL). After removal of the solvent from the former extract, the residue was washed with diethyl ether (5 mL \times 3) and dried in vacuo. The brown solid consists of a mixture of [2]Br and [3a]Br in a 5:1 molar ratio, determined by ¹H NMR spectroscopy. Removal of the solvent from the latter extract yielded a dark green solid including [1]Br₂. Further purification of each solid was not successful.

4.9. Reaction of 1 with excess Br₂ · C₄H₈O₂

To a solution of 1 (100 mg, 0.169 mmol) in CH₂Cl₂ (8 mL) was added Br₂ · C₄H₈O₂ (126 mg, 0.508 mmol) at room temperature under constant stirring. The dark green precipitates were separated by filtration and washed with CH₂Cl₂ (15 mL \times 2), then extracted with acetonitrile (30 mL). Removal of the solvent from the extract gave a dark green solid of [1](Br₃)₂. Yield: 143 mg (79%). Anal. calc. for C₂₈H₃₂Br₆Fe₄: C, 31.39; H, 3.01. Found: C, 31.04; H, 3.34%.

4.10. Reaction of 1 with BrCCl₃

A Pyrex NMR tube was charged with 1 (20 mg, 0.032 mmol), BrCCl₃ (63 mg, 0.32 mmol), and dichloromethane-*d*₂. The reaction was monitored by ¹H NMR spectroscopy.

4.11. Reaction of [2](PF₆) with H₂O

To an acetonitrile (5 mL) solution of [2](PF₆) (50 mg, 0.061 mmol) was added H₂O (0.050 mL, 2.8 mmol). After stirring for 30 min at room temperature, volatiles were removed under reduced pressure to give a mixture of [(η⁵-C₅H₄Me)₄Fe₄(μ₃-CO)(μ₃-CH)(HCCH)](PF₆) ([6](PF₆)) and [1](PF₆). The mixture was dissolved in acetonitrile (5 mL) and then treated with Cp₂Co (10 mg, 0.053 mmol) in a glovebox. After stirring the mixture for 1 h at room temperature, volatiles were removed under reduced pressure. The greenish brown residue was extracted with hexane and the extract was filtered through a Celite pad. Evaporation of the filtrate gave a brown solid of **1**. Yield: 12 mg (33%). Insoluble material on the Celite pad was extracted with dichloromethane. The solvent was removed from the extract under reduced pressure to give a dark green solid of [6](PF₆). Yield: 25 mg (54%). The identification of **1** and [6](PF₆) was performed by comparison with previous spectroscopic data.

4.12. Reaction of [2](OTf) with H₂¹⁸O

A Pyrex NMR tube was charged with [2](OTf) (20 mg, 0.024 mmol) and acetonitrile-*d*₃ (0.5 mL), followed by the introduction of H₂¹⁸O (12 mg, 0.55 mmol) into the tube under high vacuum by the trap-to-trap-transfer technique. The tube was then flame-sealed. The reaction was monitored by NMR and IR spectroscopy, revealing the clean formation of [(η⁵-C₅H₄Me)₄Fe₄(μ₃-C¹⁸O)(μ₃-CH)(HCCH)](OTf) ([6-¹⁸O](OTf)) and [1](OTf) in a 1:1 molar ratio. IR of [6-¹⁸O](OTf) (KBr) 1675 cm⁻¹ [*ν* (C¹⁸O)].

4.13. Reaction of [2](OTf) with D₂O

A Pyrex NMR tube was charged with [2](OTf) (20 mg, 0.024 mmol) and acetonitrile-*d*₃ (0.5 mL), followed by the introduction of D₂O (11 mg, 0.55 mmol) and cyclohexane (internal standard, 1 μL) into the tube under high vacuum by the trap-to-trap-transfer technique. The tube was then flame-sealed. The reaction was monitored by ¹H and ²H NMR spectroscopy, revealing the clean formation of [6](OTf) and [(η⁵-C₅H₄Me)₄Fe₄(HCCH)(HCCD)](OTf) ([1-*d*](OTf)) in a 1:1 molar ratio. ²H NMR of [1-*d*](OTf) (46.1 MHz) δ -76.3 (HCCD).

4.14. Reaction of [2](TFPB) with ZnMe₂

To a diethyl ether solution (5 mL) of [2](TFPB) (57 mg, 0.037 mmol) was added ZnMe₂ (1.0 M in hexane, 0.080 mL, 0.080 mmol) at room temperature. After stirring the solution for 10 min, volatiles were removed under reduced pressure. The residue was then washed with hexane and extracted with dichloromethane. The extract

was filtered through a Celite pad and the filtrate was concentrated to dryness in vacuo to give a brown solid of [(η⁵-C₅H₄Me)₄Fe₄(HCCH)(HCC-Me)](TFPB) ([9](TFPB)). Yield: 48 mg (88%). Anal. calc. for C₆₁H₄₆BF₂₄Fe₄: C, 49.87; H, 3.16. Found: C, 49.50; H, 3.29%. IR (KBr, cm⁻¹): 2929 (w), 1610 (w), 1489 (w), 1458 (w), 1356 (s), 1275 (vs), 1165 (s), 1124 (vs), 1092 (s), 1047 (w), 1028 (w), 885 (m), 837 (m), 820 (m), 744 (w), 715 (m), 683 (m), 669 (m). ¹H NMR (300 MHz, CD₃CN) δ -76.3 (br, *W*_{1/2} = 33 Hz, 1H, *H* CCMe), -72.8 (br, *W*_{1/2} = 37 Hz, 2H, HCCH), -27.5 (br, *W*_{1/2} = 16 Hz, 3H, HCCMe), -5.7, -0.90 (br, *W*_{1/2} = 7 Hz, 3H × 2, C₅H₄Me), -0.04 (br, *W*_{1/2} = 7 Hz, 6H, C₅H₄Me), 4.4, 4.6, 5.2, 7.6, 8.1, 9.2, 9.4, 9.8 (br, *W*_{1/2} = 14 Hz, 2H × 8, C₅H₄Me), 7.6–7.9 (br, 12H, {3,5-(CF₃)₂C₆H₃}₄B). ¹³C{¹H} NMR (75.5 MHz, CD₃CN): 7.1, 12.7, 23.0 (C₅H₄Me), 85.2, 85.3, 88.0, 92.1, 101.3, 112.1, 115.0, 119.1 (C₅H₄Me), 117.9 (TFPB), 124.8 (q, ¹*J*_{FC} = 268 Hz, TFPB), 129.4 (qq, ²*J*_{CF} = 31.3 Hz, ⁴*J*_{CF} = 3.7 Hz, TFPB), 135.0 (m, TFPB), 162.0 (q, ¹*J*_{BC} = 49.6 Hz, TFPB). ¹³C NMR signals of HCCH and HCC-Me were not assigned.

4.15. Reaction of [2](TFPB) with ZnEt₂

To a diethyl ether solution (7 mL) of [2](TFPB) (105 mg, 0.068 mmol) was added ZnEt₂ (1.0 M in hexane, 0.15 mL, 0.15 mmol) at room temperature. The solution was treated by a procedure similar to that employed in the reaction of [2](TFPB) with ZnMe₂ to give a brown solid of [(η⁵-C₅H₄Me)₄Fe₄(HCCH)(HCC-Et)](TFPB) ([10](TFPB)). Yield: 92 mg (91%). Anal. calc. for C₆₂H₄₈BF₂₄Fe₄: C, 50.21; H, 3.26. Found: C, 50.51; H, 3.27%. IR (KBr, cm⁻¹): 2965 (w), 2930 (w), 2710 (w), 2548 (w), 1610 (w), 1490 (w), 1457 (w), 1356 (s), 1276 (vs), 1168 (s), 1129 (vs), 889 (m), 838 (m), 819 (w), 714 (m), 675 (m), 667 (m). ¹H NMR (300 MHz, CD₃CN) δ -79.9 (br, *W*_{1/2} = 42 Hz, 1H, HCCCH₂CH₃), -71.4 (br, *W*_{1/2} = 40 Hz, 2H, HCCH), -37.1 (br, *W*_{1/2} = 29 Hz, 2H, HCCCH₂CH₃), -4.6 (br, *W*_{1/2} = 12 Hz, 3H, HCCCH₂CH₃), -7.4, -1.4 (br, *W*_{1/2} = 7 Hz, 3H × 2, C₅H₄Me), 5.8 (br, *W*_{1/2} = 7 Hz, 6H, C₅H₄Me), 4.2, 4.8, 7.0, 7.4, 10.0, 11.1, 12.0 (br, *W*_{1/2} = 14 Hz, 2H × 7, C₅H₄Me), 7.6–7.9 (br, 12H, {3,5-(CF₃)₂C₆H₃}₄B). ¹³C{¹H} NMR (75.5 MHz, CD₃CN): δ -2.4, 13.9, 26.1 (C₅H₄Me), -2.4 (HCCCH₂CH₃), 60.6, 77.2, 86.7, 90.5, 93.6, 103.9, 107.6, 115.9, 122.5, 133.1 (C₅H₄Me), 117.9 (TFPB), 124.7 (q, ¹*J*_{FC} = 271 Hz, TFPB), 129.1 (qq, ²*J*_{CF} = 31.0 Hz, ⁴*J*_{CF} = 2.3 Hz, TFPB), 134.9 (m, TFPB), 161.8 (q, ¹*J*_{BC} = 50.6 Hz, TFPB). ¹³C NMR signals of HCCH and HCC-Et were not assigned.

4.16. Reaction of [2](TFPB) with HC≡CMgBr

To a diethyl ether solution (20 mL) of [2](TFPB) (208 mg, 0.136 mmol) was added HC≡CMgBr (0.5 M in

THF, 0.30 mL, 0.15 mmol) at room temperature. The solution was treated by a procedure similar to that employed in the reaction of [2](TFPB) with ZnMe₂ to give a brown solid of [(η⁵-C₅H₄Me)₄Fe₄(HCCH)(HCC–C≡CH)](TFPB) ([11](TFPB)). Yield: 191 mg (95%). Anal. calc. for C₆₂H₄₄BF₂₄Fe₄: C, 50.34; H, 3.00. Found: C, 49.98; H, 3.31%. IR (KBr, cm⁻¹): 3307 (w), 2930 (w), 1741 (w), 1735 (w), 1610 (m), 1489 (w), 1356 (s), 1276 (vs), 1166 (s), 1125 (vs), 1029 (m), 886 (m), 838 (m), 822 (w), 743 (w), 715 (m), 682 (m), 669 (m). ¹H NMR (300 MHz, CD₃CN): δ -72.8 (br, W_{1/2} = 50 Hz, 2H, HCCH), -67.1 (br, W_{1/2} = 52 Hz, 1H, HCC–C≡CH), -5.5, -1.9 (br, W_{1/2} = 12 Hz, 3H × 2, C₅H₄Me), -0.90 (br, W_{1/2} = 12 Hz, 6H, C₅H₄Me), 3.9, 4.8, 5.9, 8.2, 9.2, 10.4 (br, W_{1/2} = 18 Hz, 2H × 6, C₅H₄Me), 8.9 (br, 2H × 2, accidentally overlapped, C₅H₄Me), 7.6–7.9 (br, 12H, {3,5-(CF₃)₂C₆H₃}₂B), 10.31 (s, 1H, HCC–C≡CH). ¹³C{¹H} NMR (75.5 MHz, CD₃CN): δ 10.1, 14.5, 22.0 (C₅H₄Me), 78.4, 92.7, 92.9, 105.4, 114.1, 121.0, 126.0 (C₅H₄Me), 89.7, 118.7, 126.8 (C₅H₄Me or HCC–C≡CH or HCC–C≡CH), 117.9 (TFPB), 124.7 (q, ¹J_{FC} = 271.3 Hz, TFPB), 129.2 (qq, ²J_{CF} = 31.0 Hz, ⁴J_{CF} = 3.4 Hz, TFPB), 135.0 (m, TFPB), 162.0 (q, ¹J_{BC} = 49.4 Hz, TFPB). ¹³C NMR signals of acetylenic carbons in the Fe₄C₄ core were not assigned.

4.17. Reaction of [2](PF₆) with LiS^pTol

To an acetonitrile solution of [2](PF₆) (60 mg, 0.074 mmol) was added LiS^pTol (10 mg, 0.077 mmol), and the solution was stirred for 15 min at room temperature. After removal of volatiles under vacuum, the residue was extracted with diethyl ether and the extract was filtered through a Celite pad. Evaporation of the solvent under vacuum afforded [(η⁵-C₅H₄Me)₄Fe₄(HCCH)(HCC–S^pTol)](PF₆) ([12](PF₆)). Yield: 49 mg (78%). Anal. calc. for C₃₅H₃₈F₆Fe₄PS: C, 48.93; H, 4.46. Found: C, 48.94; H, 4.65%. IR (KBr, cm⁻¹): 3115 (w), 2921 (w), 2854 (w), 1701 (w), 1684 (w), 1651 (w), 1559 (w), 1541 (w), 1481 (m), 1452 (m), 1367 (m), 1026 (m), 846 (vs), 824 (vs), 553 (s), 476 (m), 418 (m). ¹H NMR (300 MHz, CD₃CN): δ -71.4 (br, W_{1/2} = 60 Hz, 1H, HCCS^pTol), -68.0 (br, W_{1/2} = 56 Hz, 2H, HCCH), -6.4, -2.4 (br, W_{1/2} = 12 Hz, 3H × 2, C₅H₄Me), 1.39 (s, 3H, HCCSC₆H₄CH₃), 4.1, 8.5, 8.9, 10.3, 11.5, 13.1 (br, W_{1/2} = 26 Hz, 2H × 6, C₅H₄Me), 4.8 (br, W_{1/2} = 12 Hz, 6H, C₅H₄Me), 5.10, 6.35 (m, 2H × 2, HCCSC₆H₄CH₃), 5.4 (br, 2H × 2, accidentally overlapped, C₅H₄Me). ¹³C{¹H} NMR (75.5 MHz, CD₃CN): δ -3.0, 15.3, 25.1 (C₅H₄Me), 20.9 (HCCSC₆H₄CH₃), 88.2, 93.3, 107.9, 125.7, 141.9 (C₅H₄Me), 120.6, 128.7 (HCCSC₆H₄CH₃), 57.4, 77.3, 85.9, 104.6, 119.4, 136.0, 137.1, 165.0 (C₅H₄Me or HCCSC₆H₄CH₃). ¹³C NMR signals of acetylenic carbons were not assigned.

4.18. Reaction of [2](PF₆) with pyridine

A round-bottomed flask equipped with a greaseless vacuum valve was charged with [2](PF₆) (46 mg, 0.056 mmol) and acetonitrile (5 mL), followed by the introduction of pyridine (27 mg, 0.34 mmol) into the tube under high vacuum by the trap-to-trap-transfer technique. After isolating the tube off from the vacuum line, the solution was stirred for 12 h at room temperature. Volatiles were removed under reduced pressure and the residue was washed with hexane. The resulting residue was dissolved in acetonitrile and the solution was treated with NH₄PF₆ (50 mg, 0.31 mmol). After stirring for 1 h, the reaction mixture was evaporated to dryness in vacuo. The residue was washed with water and diethyl ether and then extracted with dichloromethane through a Celite pad. Removal of the solvent from the filtrate gave a brown solid of [(η⁵-C₅H₄Me)₄Fe₄(HCCH)(HCC–NC₅H₅)](PF₆)₂ ([13](PF₆)₂). Yield: 49 mg (90%). Anal. calc. for C₃₃H₃₆F₁₂Fe₄N₂P₂: C, 41.29; H, 3.78; N, 1.46. Found: C, 41.41; H, 4.07; N, 1.70%. IR (KBr, cm⁻¹): 3118 (w), 2964 (w), 2925 (w), 1618(w), 1483 (m), 1468 (m), 1375 (w), 1122 (w), 1030 (m), 841 (vs), 829 (vs), 775 (m), 731 (w), 687 (m), 557 (s). ¹H NMR (300 MHz, CD₃CN): δ -69.8 (br, W_{1/2} = 44 Hz, 2H, HCCH), -52.6 (br, W_{1/2} = 40 Hz, 1H, HCCNC₅H₅), -6.3, -2.9 (br, W_{1/2} = 12 Hz, 3H × 2, 2C₅H₄Me), 1.4 (br, W_{1/2} = 12 Hz, 6H, 2C₅H₄Me), 5.9, 6.2, 8.8, 9.1, 9.3, 10.1, 12.2, 12.8 (br, W_{1/2} = 20 Hz, 2H × 8, 4C₅H₄Me), 3.5, 4.9, 9.6 (br, HCCNC₅H₅). ¹³C{¹H} NMR (75.5 MHz, CD₃CN): 3.6, 16.7, 23.0 (C₅H₄Me), 73.1, 90.1, 94.0, 101.8, 109.1, 111.3, 118.3, 120.5, 125.5, 128.4, 129.1 (C₅H₄Me), 102.2, 126.1, 134.7 (HCCNC₅H₅). ¹³C NMR signals of acetylenic carbons were not assigned.

4.19. Reaction of [2](PF₆) with 4,4'-bipyridyl

To an acetonitrile solution of [2](PF₆) (109 mg, 0.134 mmol) was added 4,4'-bipyridyl (bpy, 22 mg, 0.14 mmol) at room temperature. The solution was stirred at 70 °C for 2 days, and then treated with NH₄PF₆ (50 mg, 0.31 mmol) at room temperature under constant stirring. After removal of volatiles under reduced pressure, the residue was washed with water, diethyl ether, and dichloromethane, and extracted with acetonitrile through a Celite pad. Evaporation of the extract under reduced pressure gave [(η⁵-C₅H₄Me)₄Fe₄(HCCH)(HCC–bpy)](PF₆)₂ ([14](PF₆)₂). Yield: 75 mg (54%). Anal. calc. for C₃₈H₃₉F₁₂Fe₄N₂P₂: C, 44.01; H, 3.79; N, 2.70. Found: C, 43.70; H, 4.06; N, 3.01%. IR (KBr, cm⁻¹): 3121 (w), 2923 (w), 1736 (w), 1717 (w), 1715 (w), 1625 (m), 1593 (w), 1482 (m), 1453 (m), 1443 (m), 1406 (m), 1372 (m), 1314 (w), 1297 (w), 1209 (w), 1118 (m), 1029 (m), 828 (vs), 555 (s). ¹H NMR (300 MHz, CD₃CN): δ -70.2 (br, W_{1/2} = 67 Hz, 2H, HCCH),

Table 8
Crystallographic Details of [2](PF₆), [4](TFPB), [5](TFPB), [9](BPh₄), [12](PF₆), [13](PF₆)₂ · 1/2CH₃CN

	[2](PF ₆) ^a	[4](TFPB) ^a	[5](TFPB) ^b	[9](BPh ₄) ^b	[12](PF ₆) ^a	[13](PF ₆) ₂ · 1/2CH ₃ CN ^a
Crystal size (mm)	0.10 × 0.03 × 0.03	0.40 × 0.40 × 0.10	0.10 × 0.10 × 0.10	0.10 × 0.10 × 0.10	0.30 × 0.20 × 0.20	0.25 × 0.15 × 0.15
Color	Greenish brown	Greenish brown	Greenish brown	Greenish brown	Greenish brown	Greenish brown
Formula	C ₂₈ H ₃₁ BrF ₆ Fe ₄ P	C ₆₀ H ₄₁ BBr ₃ F ₂₄ Fe ₄	C ₆₀ H ₄₀ BBr ₄ F ₂₄ Fe ₄	C ₅₃ H ₅₄ BFe ₄	C ₃₅ H ₃₈ F ₆ Fe ₄ PS	C ₃₄ H _{37.5} F ₁₂ Fe ₄ N _{1.5} P ₂
Formula weight	815.81	1691.86	1770.7	925.21	859.08	980.50
Crystal system	<i>Pca</i> 2 ₁	<i>P</i> 2 ₁ / <i>c</i>	<i>P</i> 2/ <i>c</i>	<i>P</i> $\bar{1}$	<i>P</i> 2 ₁ / <i>c</i>	<i>P</i> 2 ₁
Space group	Orthorhombic	Monoclinic	Monoclinic	Triclinic	Monoclinic	Monoclinic
<i>a</i> (Å)	28.125(6)	13.4496(3)	12.4977(7)	10.1333(3)	18.8044(1)	12.1054(6)
<i>b</i> (Å)	13.870(3)	17.3820(6)	12.4868(5)	13.0520(3)	18.8922(4)	14.1386(7)
<i>c</i> (Å)	14.430(3)	25.1948(6)	19.579(1)	16.0867(6)	18.7111(1)	21.0710(11)
α (°)	90	90	90	97.6408(8)	90	90
β (°)	90	92.7598(10)	102.338(1)	95.5324(8)	150.9437(5)	92.868(3)
γ (°)	90	90	90	94.054(1)	90	90
Volume (Å ³)	5629.2(19)	5883.2(3)	2984.8(3)	2091.4(1)	3228.35(7)	3601.9(3)
<i>Z</i>	8	4	2	2	4	4
μ (mm ⁻¹)	3.556	3.122	3.754	1.396	1.937	1.759
Reflections collected	42993	44758	25268	20479	27448	28029
Independent reflections (<i>R</i> _{int})	12623 (0.0730)	12752 (0.062)	6775 (0.042)	9506 (0.069)	7088 (0.0297)	14608 (0.0869)
Maximum and minimum transmission	0.9008 and 0.7175	0.3682 and 0.7454	0.5034 and 0.6870	0.8673 and 0.9181	0.5941 and 0.6979	0.7269 and 0.9225
GOF on <i>F</i> ²	1.035	1.017	1.61	1.15	1.134	1.135
Final <i>R</i> indices [<i>I</i> > 2σ(<i>I</i>)]	<i>R</i> ₁ = 0.0703, <i>wR</i> ₂ = 0.1574	<i>R</i> ₁ = 0.0997, <i>wR</i> ₂ = 0.2590	<i>R</i> ₁ = 0.058	<i>R</i> ₁ = 0.075	<i>R</i> ₁ = 0.0261, <i>wR</i> ₂ = 0.0893	<i>R</i> ₁ = 0.0634, <i>wR</i> ₂ = 0.1605
<i>R</i> indices (all data)	<i>R</i> ₁ = 0.0975, <i>wR</i> ₂ = 0.1736	<i>R</i> ₁ = 0.1320, <i>wR</i> ₂ = 0.2886	<i>R</i> = 0.085, <i>R</i> _w = 0.166	<i>R</i> = 0.122, <i>R</i> _w = 0.298	<i>R</i> ₁ = 0.0309, <i>wR</i> ₂ = 0.1070	<i>R</i> ₁ = 0.0763, <i>wR</i> ₂ = 0.1730
Largest difference peak and hole (e Å ⁻³)	2.168 and -1.308	2.19 and -1.53	1.90 and -0.80	1.16 and -0.69	0.684 and -0.726	0.942 and -0.952

^a Calculated by using SHELXS-97 and SHELXL-97. $R_1 = \sum |F_o|^2 - |F_c|^2| / \sum |F_o|^2$; $wR_2 = [\sum w(F_o^2 - F_c^2)^2 / \sum w(F_o^2)^2]^{1/2}$, where $w = q[\sigma^2(F_o^2) + (ap)^2 + bp]^{-1}$.

^b Calculated by using the teXsan package. $R_1 = \sum ||F_o| - |F_c|| / \sum |F_o|$ for $I > 3.0\sigma(I)$; $R = \sum (F_o^2 - F_c^2) / \sum F_o^2$; $R_w = [\sum w(F_o^2 - F_c^2)^2 / \sum w(F_o^2)^2]^{1/2}$.

–52.9 (br, $W_{1/2} = 50$ Hz, 1H, $HCC(NC_{10}H_8N)$), –6.3, –3.0 (br, $W_{1/2} = 20$ Hz, $3H \times 2$, C_5H_4Me), 2.0 (br, $W_{1/2} = 20$ Hz, 6H, C_5H_4Me), 6.0, 6.1, 8.8, 9.2, 9.4, 10.4, 12.5, 13.0 (br, $W_{1/2} = 42$ Hz, $2H \times 8$, C_5H_4Me), 3.6, 4.9, 7.5, 8.4 (br, $2H \times 4$, $HCC(NC_{10}H_8N)$). $^{13}C\{^1H\}$ NMR (75.5 MHz, CD_3CN): δ 3.1, 16.9, 22.9 (C_5H_4Me), 70.7, 88.5, 93.9, 101.8, 106.2, 108.6, 122.8 (C_5H_4Me), 102.9, 132.9, 154.4 ($HCC(NC_{10}H_8N)$). ^{13}C NMR signals of acetylenic carbons were not assigned.

4.20. Reactions of [2](PF₆) with 4,4'-bipyridyl in the presence of AgOTf

To a solution of [2](PF₆) (78 mg, 0.096 mmol) in acetonitrile (5 mL) was added AgOTf (31 mg, 0.12 mmol) at room temperature. The solution was stirred for 5 min, treated with 4,4'-bipyridyl (20 mg, 0.13 mmol), and then stirred for a further 30 min. Volatiles were removed under vacuum and the residue was extracted with acetonitrile. The extract was treated with NH₄PF₆ (30 mg, 0.18 mmol) at room temperature and stirred for 30 min. After removal of volatiles, the residue was washed with water, diethyl ether, and then dichloromethane, and further extracted with acetonitrile. Removal of the solvent from the extract gave a brown solid of [14](PF₆)₂. Yield: 89 mg (90%).

4.21. X-ray crystallography

The counter anions of [4](OTf) and [5](OTf) were replaced with TFPB by dissolving [4](OTf) or [5](OTf) and NaTFPB in acetonitrile. The counter anion of [9](TFPB) was replaced with BPh₄[–] by dissolving [9](TFPB) and NaBPh₄ in acetonitrile. Single crystals of [2](PF₆) were obtained from the CH₂Cl₂/diethyl ether solution at room temperature. Single crystals of [4](TFPB), [5](TFPB), [9](BPh₄), and [12](PF₆) were obtained from the CH₂Cl₂/hexane solutions at room temperature. Crystals of [13](PF₆)₂ were grown at room temperature by placing a layer of diethyl ether over an acetonitrile solution of [13](PF₆)₂. Intensity data were collected at 150 K on a RIGAKU RAXIS-RAPID Imaging Plate diffractometer with graphite monochromated Mo K α radiation.

The structures of [5](TFPB) and [9](BPh₄) were solved by heavy-atom Patterson methods (PATTY) and expanded using Fourier techniques (DIRDIF94). All calculations were performed using the teXsan crystallographic software package of Molecular Structure Corporation. The structures of [2](PF₆), [4](TFPB), [12](PF₆), and [13](PF₆)₂ were solved by Patterson and Fourier transform methods using SHELXS-97 and refined by full-matrix least-squares techniques on all F^2 data (SHELXL-97) [14]. The hydrogen atoms were partially located from difference electron-density maps, and the rest were fixed at the calculated positions.

Some details of data collection and refinement are given in Table 8.

5. Supplementary material

Crystallographic data for the structure analysis have been deposited with the Cambridge Crystallographic Data Center, CCDC Nos. 261949 ([2](PF₆)), 261950 ([4](TFPB)), 247239 ([5](TFPB)), 247240 ([9](BPh₄)), 261951 ([12](PF₆)), and 247241 ([13](PF₆)₂ · 1/2CH₃CN). Copies of this information may be obtained free of charge from the Director, CCDC, 23 Union Road, Cambridge CB2 1EZ, UK (fax: +44 1223 336 033; e-mail: deposit@ccdc.cam.ac.uk or www: <http://www.ccdc.cam.ac.uk>).

References

- [1] (a) L. Brandsma, Preparative acetylenic chemistry, Elsevier, New York, 1971; (b) S. Patai, Supplement C2: the chemistry of triple-bonded functional groups, Wiley, New York, 1991 (Chapter 6); (c) A. Wagner, M.P. Heitz, C. Mioskowski, Tetrahedron Lett. 31 (1990) 3141; (d) P. Vinczer, S. Struhar, L. Novak, C. Szantay, Tetrahedron Lett. 33 (1992) 683; (e) I. Nishiguchi, O. Kanbe, K. Itoh, H. Maekawa, Synlett (2000) 89, and references cited therein.
- [2] (a) C.G. Krespan, J. Org. Chem. 40 (1975) 261; (b) K. Stahl, A. El-Kholi, U. Müller, K. Dehnicke, J. Organomet. Chem. 316 (1986) 95; (c) R.G. Beevor, M. Green, A.G. Orpen, I.D. Williams, J. Chem. Soc., Dalton Trans. (1987) 1319; (d) K. Sünkel, J. Organomet. Chem. 348 (1988) C12; (e) D. Lentz, H. Michael, Angew. Chem., Int. Ed. Engl. 27 (1988) 845; (f) C. Löwe, H.-U. Hund, H. Berke, J. Organomet. Chem. 371 (1989) 311; (g) K. Sünkel, U. Birk, C. Robl, Organometallics 13 (1994) 1679; (h) K. Sünkel, U. Birk, Polyhedron 18 (1999) 3187; (i) H. Lang, G. Rheinwald, U. Lay, L. Zsolnai, G. Huttner, J. Organomet. Chem. 634 (2001) 74.
- [3] (a) M. Okazaki, T. Ohtani, S. Inomata, N. Tagaki, H. Ogino, J. Am. Chem. Soc. 120 (1998) 9135; (b) M. Okazaki, T. Ohtani, M. Takano, H. Ogino, Inorg. Chem. 41 (2002) 6726; (c) M. Okazaki, T. Ohtani, H. Ogino, J. Am. Chem. Soc. 126 (2004) 4104; (d) M. Okazaki, T. Ohtani, M. Takano, H. Ogino, Organometallics 23 (2004) 4055.
- [4] M. Takano, M. Okazaki, H. Tobita, J. Am. Chem. Soc. 126 (2004) 9190.
- [5] J.A. Dean, Lange's handbook of chemistry, McGraw-Hill, New York, 1999.
- [6] E. Boyar, A.J. Deeming, S.E. Kabir, J. Chem. Soc., Chem. Commun. (1986) 577.
- [7] K.P.C. Vollhardt, M. Wolfgruber, Angew. Chem., Int. Ed. Engl. 25 (1986) 929.
- [8] (a) Y.S. Wong, H.N. Paik, P.C. Chieh, A.J. Carty, J. Chem. Soc., Chem. Commun. (1975) 309; (b) A.J. Deeming, S. Hasso, J. Organomet. Chem. 112 (1976) C39;

- (c) A.J. Carty, N.J. Taylor, W.F. Smith, *J. Chem. Soc., Chem. Commun.* (1978) 1017;
(d) A.J. Carty, G.N. Mott, N.J. Taylor, J.E. Yule, *J. Am. Chem. Soc.* 100 (1978) 3051;
(e) A.J. Carty, G.N. Mott, N.J. Taylor, *J. Organomet. Chem.* 182 (1979) C69;
(f) E. Sappa, A. Tiripicchio, P. Braunstein, *Chem. Rev.* 83 (1983) 203.
- [9] S. Kiviniemi, M. Nissinen, T. Alaviuhkola, K. Rissanen, J. Pursiainen, *J. Chem. Soc., Perkin Trans. 2.* (2001) 2364.
- [10] (a) F. Paul, C. Lapinte, Unusual structures and physical properties in organometallic chemistry, in: M. Gielen, R. Willem, B. Wrackmeyer (Eds.), Wiley, New York, 2002, pp. 220–291;
(b) S. Szafert, J.A. Gladysz, *Chem. Rev.* 103 (2003) 4175;
(c) M. Akita, A. Sakurai, M.-C. Chung, Y. Moro-oka, *J. Organomet. Chem.* 670 (2003) 2;
(d) M.I. Bruce, P.J. Low, *Adv. Organomet. Chem.* 50 (2004) 179;
(e) Q. Zheng, F. Hampel, J.A. Gladysz, *Organometallics* 23 (2004) 5896;
(f) S. Roué, C. Lapinte, *J. Organomet. Chem.* 690 (2005) 594.
- [11] (a) T. Ito, T. Hamaguchi, H. Nagino, T. Yamaguchi, J. Washington, C.P. Kubiak, *Science* 277 (1997) 660;
(b) T. Ito, T. Hamaguchi, H. Nagino, T. Yamaguchi, H. Kido, I.S. Zavarine, T. Richmond, J. Washington, C.P. Kubiak, *J. Am. Chem. Soc.* 121 (1999) 4625;
(c) T. Ito, N. Imai, T. Yamaguchi, T. Hamaguchi, C.H. Londergan, C.P. Kubiak, *Angew. Chem. Int. Ed.* 43 (2004) 1376;
(d) M. Fujita, M. Tominaga, A. Hori, B. Therrien, *Acc. Chem. Rec. ASAP.*
- [12] G.R. Allan, S.J. Rychnovsky, C.H. Venzke, T.F. Boggess, L. Tutt, *J. Phys. Chem.* 98 (1994) 216.
- [13] (a) G. Wilkinson, F.A. Cotton, J.M. Birmingham, *J. Inorg. Nucl. Chem.* 2 (1956) 96;
(b) R.B. King (Ed.), *Organometallic syntheses*, vol. 1, Academic Press, New York, 1965, p. 70.
- [14] (a) G.M. Sheldrick, *SHELXS-97*, Programs for solving X-ray crystal structures, University of Göttingen, 1997;
(b) G.M. Sheldrick, *SHELXL-97*, Programs for refining X-ray crystal structures, University of Göttingen, 1997.